

Operando Spectroscopy in Catalytic Carbonylation Reactions

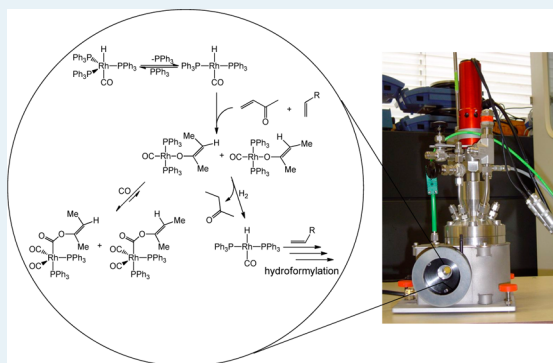
Olivier Diebolt,[†] Piet W. N. M. van Leeuwen,[†] and Paul C. J. Kamer^{*,‡}

[†]Institute of Chemical Research of Catalonia (ICIQ), Av. Paisos Catalans, 16, 43007 Tarragona, Spain

[‡]EaSTCHEM, School of Chemistry, University of St. Andrews, St. Andrews, Fife, KY16 9ST, United Kingdom

ABSTRACT: Over the years, *in situ* spectroscopic studies have contributed largely to an in-depth mechanistic understanding of many homogeneously catalyzed reactions. This review discusses the application of operando spectroscopy such as high pressure infrared and NMR to obtain in-depth mechanistic understanding of transition metal catalyzed carbonylation reactions. Several catalytic reactions of industrial relevance are discussed including rhodium catalyzed hydroformylation, palladium catalyzed alkoxy carbonylation, and copolymerization of CO and alkenes. Also, mechanistic studies of tandem reactions such as rhodium catalyzed hydroaminomethylation and hydroformylation-hydrogenation are included. In addition, the effects of alternative media such as supercritical CO₂ and ionic liquids are discussed.

KEYWORDS: homogeneous catalysis, *in situ* spectroscopy, HP-NMR, HP-IR, operando spectroscopy, carbonylation, hydroformylation



1. INTRODUCTION

Since the discovery of the Wilkinson hydrogenation catalyst, [RhCl(PPh₃)₃],¹ a rapidly growing number of phosphine ligands has been applied in many catalytic reactions. Soon it became obvious that the steric and electronic properties of the ligands appeared to have a large effect on the reactivity of the catalytic transition metal complexes. As it became evident that the reactivity of organotransition metal complexes is dependent on the ligand environment of the metal, a search for a systematic classification of ligand properties was initiated. Several parameters have been developed to quantify the electronic and steric properties of ligands. Tolman used the A₁ stretching vibration frequencies of [Ni(CO)₃L] complexes to define an electronic parameter (χ) for phosphorus ligands, using P(*t*-Bu)₃ as a reference ligand.² The overall electronic ligand properties are merely a combination of σ -donation and π -acidity. Several attempts have been made to separate these entangled electronic parameters leading to Drago's definition of two parameters E_B and C_B, for phosphine reactivity, indicating electrostatic and covalent contributions, respectively.^{3,4} Giering and Prock described a quantitative analysis of ligand effects (QALE), which is derived from several physical properties of metal complexes.^{5,6} Giering described the electronic properties of a ligand by three electronic parameters: σ -donor capacity (χ_d), π -acidity (π_p), and an aryl effect (E_{ar}).

Tolman also introduced one of the most applied concepts of quantifying the steric congestion that a ligand causes, the cone angle (θ).⁷ Tolman took a typical Ni–phosphorus distance of 2.28 Å as standard to construct a cone from the metal center that embraces all the atoms in the ligand based on CPK models. In general, the Tolman cone angle overestimates the real steric congestion and several approaches have been developed to provide a more accurate description of steric bulk such as

White's solid angle,⁸ Brown's steric repulsive parameter E_R,⁹ Barron's pocket angle,¹⁰ Leitner's accessible molecular surface,¹¹ and Cavallo's buried volume %V_{Bur}.^{12–14} As most of these methods require laborious input from computational or crystallographic data, the Tolman cone angle is often still used despite its limitations.

Chelating ligands have a striking effect on the conformation and stability of transition metal complexes and consequently on the catalytic reactivity. Thorn and Hoffmann already predicted that geometrical constraints could affect the reactivity of metal complexes strongly.¹⁵ Their theoretical work showed that during migration in a square planar palladium diphosphine complex the P–M–P angle would widen in order to “pursue” the migrating group. In a reversed manner, it was reasoned that ligands enforcing an enlarged P–M–P angle would resemble the transition state and result in faster migration reactions. Dekker et al. provided experimental support by showing that larger bite angles of palladium diphosphine complexes resulted in increased migration rates.¹⁶ Casey and Whiteker introduced the concepts of the natural bite angle and the flexibility range for diphosphine ligands.¹⁷ The natural bite angle proved to be a powerful tool to predict conformational preferences of bidentate ligands. More rigid backbones cannot only support but actually enforce a coordination angle that will stabilize or destabilize a certain coordination mode. This will have impact on an elementary reaction step of a catalytic cycle in several

Special Issue: Operando and In Situ Studies of Catalysis

Received: July 16, 2012

Revised: September 22, 2012

Published: September 25, 2012

ways, i.e., stabilization or destabilization of the initial, transition, or final state.¹⁸

While the increasing knowledge about organotransition metal compounds and computational chemistry has provided fundamental knowledge of the factors influencing elementary reaction steps, catalyst development is still hampered by lack of insight in the transition state of the selectivity-determining step. Furthermore, in general a catalytic transformation consists of several elementary steps that will be influenced in different ways by ligand modifications. Therefore, rational design of ligands, in particular for enantioselective transformations, is still a challenging task and requires better understanding of the structure and reactivity of catalytic intermediates. Nevertheless, optimizing the catalytic center by varying the ligand properties is a powerful tool in homogeneous catalysis.¹⁹ Impressive results have been obtained in both small-scale (asymmetric) catalytic preparation of fine-chemicals and industrial production of bulk-chemicals. Intimate knowledge of the concentration, structure, and reactivity of organometallic intermediates of a catalytic cycle under real reaction conditions can provide valuable information which can eventually lead to more efficient rational catalyst design.

In situ analysis of the organometallic species present in solution under catalytic conditions is a very powerful tool to get insight into the coordination mode, identification of the active species, and better understanding of the catalytic cycle and the catalytic outcome.^{20,21} These powerful tools allowed to identify the active species leading to high regioselectivities and eventually enantioselectivities. Lately, these techniques, mainly consisting of *in situ* high-pressure NMR (HPNMR) and *in situ* high-pressure infrared (HPIR), have been used in order to better understand the role of new ligands under catalytic conditions and in particular their coordination modes. It is important to note that isotopic labeling studies have also proven powerful, but these will not be discussed here.

High-pressure NMR is a powerful technique for the identification of organometallic compounds, providing very detailed structural information.^{22,23} Roe performed a detailed mechanistic study on CO exchange in cobalt carbonyl complexes, which is an early example of the use of high-pressure sapphire NMR tubes in organometallic chemistry and homogeneous catalysis. He showed that CO exchange from solution with $\text{Co}_2(\text{CO})_8$ was independent of CO pressure.²⁴ Also, the exchange between CO in solution and the terminal carbonyls of $\text{CH}_3\text{C}(\text{O})\text{Co}(\text{CO})_4$ was independent of the CO concentration, whereas the exchange of the carbonyl moiety in the acetyl group required deinsertion, and this was strongly inhibited by increasing CO pressure. The high-pressure sapphire NMR tube is a convenient tool for comparing catalyst resting states in alternative media with traditional organic solutions to detect media effects on catalyst structure and equilibria. Horvath showed that fluororous phase hydroformylation catalyst $\text{HRh}(\text{CO})_x[\text{PCH}_2\text{CH}_2(\text{CF}_2)_5\text{CF}_3]_{4-x}$ was an equilibrium between the species with $x = 2$ and $x = 1$ depending on CO and ligand concentration in a similar way as the organic triphenylphosphine analogue.²⁵ Elsevier et al. modified Roe's sapphire tube by adding a pressure sensor.²⁶ Using this cell, they could explain the change of selectivity from cyclic amides to cyclic amines in the rhodium-catalyzed hydroaminomethylation of ethyl methallylic amine when changing from organic solvent to supercritical CO_2 .²⁷ The solvent CO_2 was also acting as a temporary protecting group by forming carbamates of the amine intermediates.

NMR is a relatively slow and insensitive spectroscopic tool. Consequently, relatively high concentrations are required to obtain acceptable signal-to-noise ratios. In special cases, sensitivity problems can be solved using special methods such as ParaHydrogen Induced Polarization NMR (PHIP), which is a very powerful technique when dihydrogen is involved in a catalytic reaction.^{28–30} Small gas volumes and long diffusion times in high-pressure NMR tubes prevent following fast catalytic reactions with gaseous substrates under real catalytic conditions. Special flow cells have been developed by Iggo³¹ and Selent,³² which prevent mass-transfer limitations, but still high concentrations are required which are in general different from real catalytic conditions. Infrared spectroscopy has a much faster time scale and is much more sensitive than NMR and, therefore, offers better prospects for fast reactions at low catalyst concentrations. Especially in the case where the catalytic species is a transition metal carbonyl complex, the strong CO vibrations provide an excellent analytical tool for studying the intermediate species. Hence, important carbonylation reactions such as rhodium catalyzed hydroformylation can be studied at actual catalytic conditions involving low concentrations and high temperatures and pressures. One of the first high-pressure autoclaves for infrared measurements was described by Noack as early as 1968.³³ The catalytic reaction mixture content of an external high-pressure autoclave was continuously pumped through a high-pressure transmission cell. The disadvantage of this system is the time delay between the sample leaving the autoclave and reaching the infrared cell. In the case of fast reactions, this will lead to gas depletion and the actual measured sample might differ from the actual catalytic reaction mixture. A solution was provided by Moser et al. who embedded a cylindrical internal reflection crystal (CIR) into a standard Parr Mini Reactor.^{34,35} This is an elegant setup for real *in situ* measurements which has found a lot of follow-up in the form of flexible inlet probes containing a CIR. A major disadvantage of these systems is the small penetration depth of the signal into the solution resulting in relatively bad signal-to-noise ratios. A good compromise between time delay and sensitivity is provided by the fast *in situ* infrared transmission cell developed by van Leeuwen et al.²¹

An early example of the use of HPIR to provide mechanistic insight under real catalytic conditions was provided by Whyman. He used his *in situ* HPIR cell^{36,37} to study the cobalt carbonyl catalyzed hydroformylation of olefins under high pressures and temperatures and found that depending on the nature of alkene substrate and ligand, CO or PBU_3 , the resting state of the catalytic system changed from acyl cobalt to hydrido cobalt carbonyl.³⁸

Although IR is already a fast and sensitive technique compared to, for example, NMR, the sensitivity and analysis of complex mixtures can be even further enhanced by applying sophisticated algorithms such as band-target entropy minimization (BTEM).^{39,40} Garland applied this algorithm to identify the compounds present during $\text{HMn}(\text{CO})_5$ promoted $\text{Rh}_4(\text{CO})_{12}$ catalyzed hydroformylation.⁴¹ Detailed analysis of all intermediates present and the kinetics of the reaction indicated that next to the classic unicyclic mechanism involving reaction with H_2 , an additional mechanism was operative involving bimetallic catalytic binuclear elimination. In a subsequent study using $\text{HRe}(\text{CO})_5$ as a promotor, they confirmed the presence of bimetallic intermediates.⁴² This promoting effect of the bimetallic mechanism leading to large

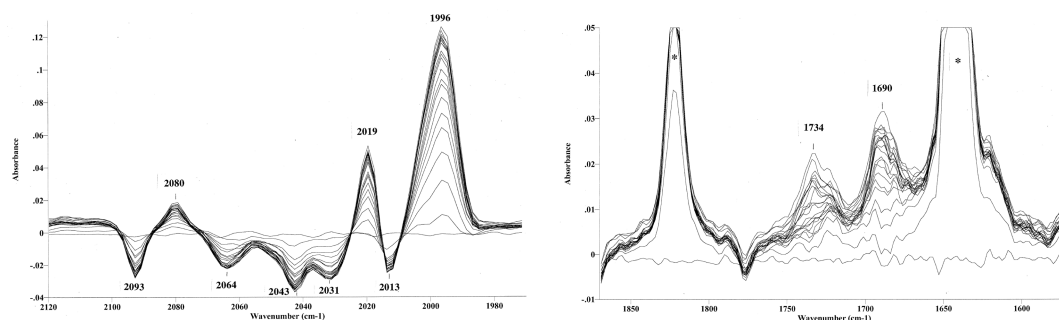


Figure 1. Terminal CO (left) and acyl (right) regions of IR spectra recorded with the rapid-scan method after addition of oct-1-ene to $[\text{RhH}(\text{CO})_3\text{P}]$ ($\text{P} = \text{tris}(2\text{-tert-butyl-4-methylphenyl})$ phosphite). * = oct-1-ene. Reprinted with permission from ref 21. Copyright 2004 Elsevier.

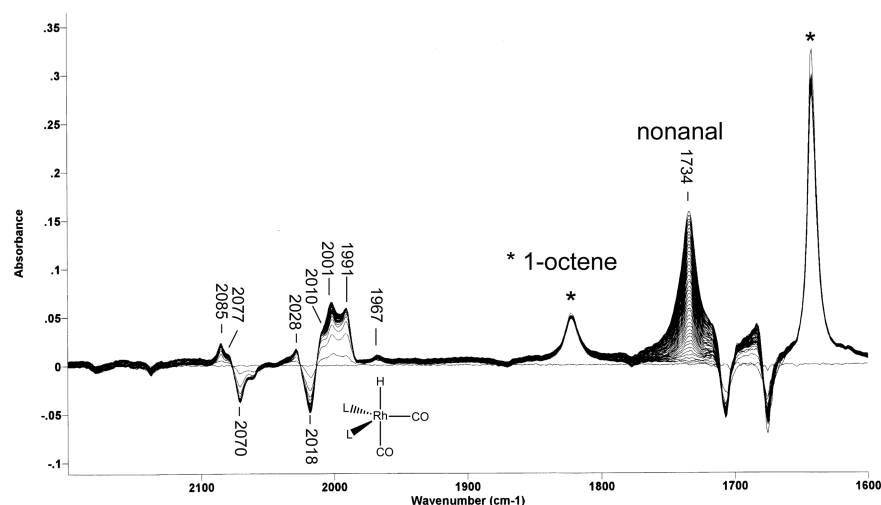


Figure 2. Difference IR spectrum of $[\text{RhH}(\text{CO})_2\text{L}_2]$ after addition of oct-1-ene substrate. Reprinted from ref 47. Copyright 2001 American Chemical Society.

rate enhancements by addition of metal hydrides seemed to be quite general and operative for different alkene substrates.⁴³

2. HYDROFORMYLATION IN ORGANIC SOLVENTS

Van Leeuwen et al. used their HPIR cell to study their very fast bulky phosphite modified rhodium hydroformylation catalyst.⁴⁴ This catalyst showed extremely high turnover rates of 40 000 mol $[\text{mol Rh}]^{-1} \text{h}^{-1}$ ($P = 20$ bar H_2/CO , $T = 80$ °C, 0.002 mmol of $[\text{Rh}]$, 0.1 mmol of tris(2-*tert*-butyl-4-methyl)phenyl phosphite, 20 mmol of oct-1-ene in 20 mL of toluene). Also the rate equation differed from the usual triphenylphosphine modified rhodium catalyzed hydroformylation reactions with a zeroth order rate dependency of the oct-1-ene concentration. In addition, a first order dependency on the dihydrogen pressure was observed which suggested a rate limiting hydrogenolysis of the rhodium acyl intermediate. Jongsma et al. had already shown that the active hydroformylation catalyst based on a similar bulky phosphite contains only one phosphite under actual reaction conditions, which explained the high rates.⁴⁵ For NMR studies of a bulky phosphite based catalyst, see the later work by Roodt et al.⁴⁶ Detailed studies by van Leeuwen et al. using the *in situ* HPIR cell for rapid scan measurements showed that for 1-alkenes as substrates a rhodium acyl complex containing one phosphite ligand was indeed the resting state of the catalytic cycle.²¹ The three carbonyl vibrations of the initial rhodium hydride shifted to higher frequencies, and for a short period the Rh–acyl CO vibration was visible at 1690 cm^{-1} before it was completely

obscured by the product aldehydes signal (see Figure 1). This corroborated the kinetic studies which already indicated that hydrogenolysis of the rhodium acyl complex was the rate limiting step.

In a subsequent study, the same group investigated the mechanism of the rhodium catalyzed hydroformylation using *N*-acyl phosphorus diamides, bulky and strongly π -accepting ligands.⁴⁷ Analogous to bulky phosphites, the stronger electron withdrawing properties and increased steric bulk lead to higher hydroformylation rates compared to phosphine-based catalyst systems.⁴⁸ Investigation of the rhodium complexes formed under hydroformylation reaction conditions revealed that the monodentate ligands form mixtures of $[\text{RhH}(\text{CO})_2\text{L}_2]$ and $[\text{RhH}(\text{CO})_3\text{L}]$. The ratio $[\text{RhH}(\text{CO})_2\text{L}_2]/[\text{RhH}(\text{CO})_3\text{L}]$ depends on the ligand concentration and its bulkiness. The kinetic rate equation, $v = k[\text{oct-1-ene}]^{0.3}[\text{L}]^{-0.3}[\text{CO}]^{-1}[\text{Rh}]^1[\text{H}_2]^{0.8}$, and (*in situ*) spectroscopic techniques revealed that several of the elementary reaction steps are involved in the hydroformylation rate control. Depending on the exact reaction conditions, the rate determining step shifted from alkene addition/hydride migration at low alkene concentration and high H_2 pressure to hydrogenolysis of the Rh–acyl at high alkene concentration and low H_2 pressure. Deuterioformylation showed that alkene coordination followed by hydride migration is irreversible under the conditions studied. The rhodium–hydride complex $[\text{RhH}(\text{CO})_2\text{L}_2]$ could be formed *in situ* from the $[\text{Rh}(\text{acac})(\text{CO})_2]$ precursor, and several rhodium–acyl

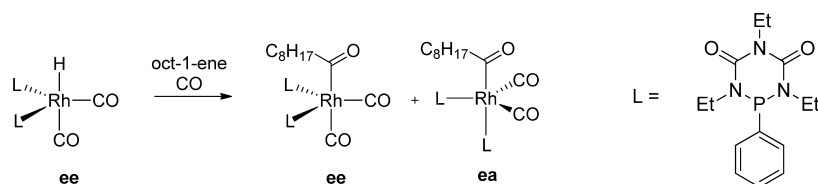


Figure 3. ee - $[\text{RhH}(\text{CO})\text{L}_2]$ forms ee and ea acyl-complexes.

complexes were formed after addition of the alkene substrate according to *in situ* HPIR spectroscopy (see Figure 2).

The structures of the rhodium–acyl complexes have been further characterized using ^{31}P , ^{13}C , and ^{103}Rh NMR spectroscopy. The rhodium–hydride complex contained two phosphorus ligands which were exclusively coordinated in the equatorial plane. The rhodium–acyl complexes formed under the actual hydroformylation conditions contained phosphorus ligands coordinated in both the bisequatorial (ee) and equatorial-axial (ea) coordination modes (see Figure 3).

Most phosphine-based rhodium hydroformylation catalysts have a rate limiting step early in the catalytic cycle. Kinetic studies do not easily distinguish between the three individual steps of CO dissociation, alkene addition, and hydride migration. The rate of CO dissociation was investigated by van Leeuwen et al. for a series of diphosphine ligands from the Xantphos family by ^{13}C O labeling experiments using rapid-scan IR (see Figure 4).⁴⁹

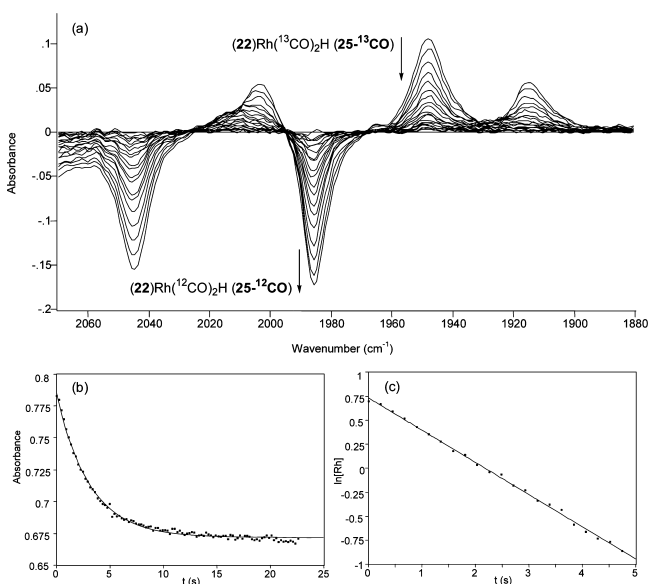


Figure 4. Difference HPIR spectrum (a) and kinetic data (b and c) for the ^{13}C O dissociation from $[\text{RhH}(\text{CO})_2(\text{diphosphine})]$ in the presence of ^{12}C O at 40°C . Reprinted from ref 49. Copyright 1999 American Chemical Society.

The ^{13}C O in $[\text{RhH}(\text{CO})_2(\text{diphosphine})]$ complexes can be exchanged for ^{12}C O. This CO exchange process obeys simple first-order kinetics as it follows a dissociative mechanism. The CO dissociation rate constants k_1 can be obtained by following the disappearance of the ^{13}C O vibration from the $[\text{RhH}(\text{CO})_2(\text{diphosphine})]$ complex by rapid-scan HPIR spectroscopy. After loading the ^{13}C O complex, the exchange was started by applying a high pressure of ^{12}C O and the CO vibration of the complex at 1945 cm^{-1} started to decrease in intensity (see Figure 4) as the concentration of the complex diminished. The

change in concentration was used to derive the kinetic data of the exchange reaction and the k_1 of the CO dissociation. The linear logarithmic plot of the complex concentration in time indicates that the CO dissociation of the $[\text{RhH}(\text{CO})_2(\text{diphosphine})]$ complexes in time follows simple first-order kinetics. The negative of the slope of this line is the first-order rate constant k_1 . It was found that the rate of CO dissociation at 40°C was higher than the overall hydroformylation rate at 80°C , indicating that CO dissociation is about 2 orders of magnitude faster than the catalytic reaction.

Van Leeuwen et al. performed an *in situ* mechanistic study to the deactivation of hydroformylation catalysts. As model reactions, they performed controlled reactions of the common intermediate hydroformylation catalyst $[\text{RhH}(\text{CO})_2(\text{PPh}_3)_2]$ with likely impurities in alkene feeds such as dienes, alkynes, and enones.⁵⁰ The hydrido rhodium complex $[\text{RhH}(\text{CO})_2(\text{PPh}_3)_2]$ is the common catalyst resting state under actual hydroformylation conditions. This compound was prepared in an HPIR autoclave and reacted with 3-buten-2-one (MVK) as a model substrate for unsaturated ketones. Immediately after addition, two new bands were formed in the IR spectrum and the four bands of $[\text{RhH}(\text{CO})_2(\text{PPh}_3)_2]$ disappeared (Figure 5). Interestingly, when most of MVK had reacted, $[\text{RhH}(\text{CO})_2(\text{PPh}_3)_2]$ was regenerated and became again the predominant species. Additional HPNMR studies showed that enones react with the rhodium hydride to form rhodium enolate intermediates which formed carboalkoxy–rhodium complexes under CO pressure. Slow decarbonylation followed by hydrogenation to butanone resulted in regeneration of the active rhodium hydride intermediate.

Selent and co-workers reported in 2010 the use of phosphite-modified rhodium catalysts for the hydroformylation of neohexene (3,3-dimethyl-1-butene).⁵¹ *In situ* spectroscopy during the catalyst preformation period allowed for better understanding of these systems. Bulky acyl-bidentate ligand **1** and monodentate ligand **2** were used (see Figure 6).

The reactivity of $[\text{Rh}(\text{acac})(\text{CO})_2]$ and **1** ($[\text{Rh}] = 1.11\text{ mM}$, $\text{Rh}/\text{L} = 1:4$) in the presence of 2 MPa syngas pressure was investigated (see Figure 7). The rhodium precursor and the ligand rapidly reacted to form the complex $[\text{Rh}(\text{acac})(\text{1})]$. When syngas pressure was applied, complete dissociation of the ligand was observed first, forming again the starting rhodium precursor. This effect has also been observed for other types of ligands. After ~ 20 min of reaction at 70°C , appearance of new peaks in the IR spectrum showed the formation of pentavalent ea -hydrido rhodium complex, $[\text{RhH}(\text{CO})_2(\text{1})]$, which was the only detectable intermediate during the catalytic reaction after addition of substrate. This appeared to be the main catalyst resting state, and dissociation of a carbon monoxide molecule from this complex seemed the rate limiting step in catalysis.

The authors conducted the same experiments using monodentate ligand **2** (see Figure 8). In this case, mixing the ligand with the rhodium precursor gave the monoligated complex $[\text{Rh}(\text{acac})(\text{CO})(\text{2})]$. As in the case of the bidentate

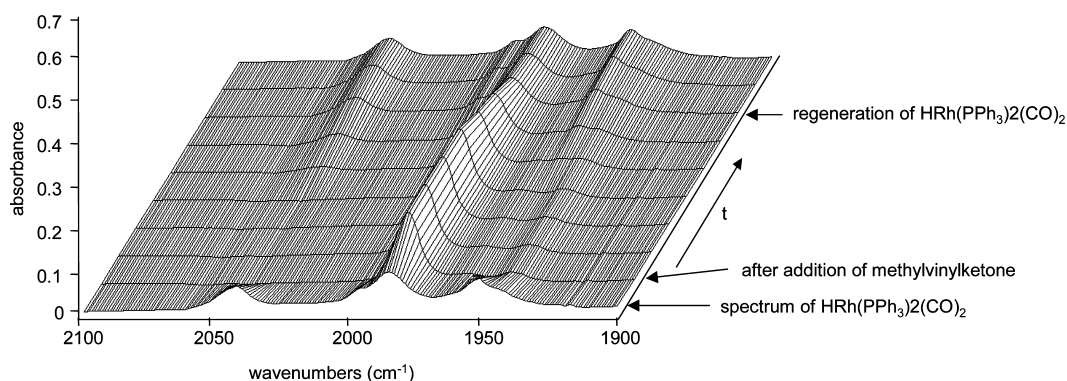


Figure 5. *In situ* HPIR study of the reaction of $[\text{RhH}(\text{CO})_2(\text{PPh}_3)_2]$ with methylvinylketone. Reprinted with permission from ref 50. Copyright 2003 Wiley-VCH Verlag GmbH & Co. KGaA.

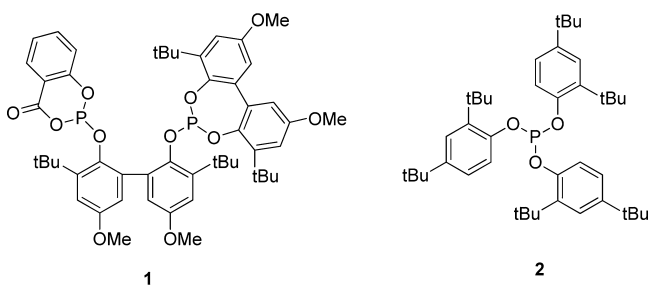


Figure 6. Ligands 1 and 2.

phosphite, addition of syngas resulted first in the formation of the starting complex $[\text{Rh}(\text{acac})(\text{CO})_2]$ and the slower formation of the well-known monodentate hydride species $[\text{RhH}(\text{CO})_3(\mathbf{2})]$. Interestingly, in this instance, upon addition of the substrate neohexene, a new complex was detected, being the acyl complex $[\text{Rh}\{-\text{C}(\text{O})-(\text{CH}_2)_2-\text{C}(\text{CH}_3)_3\}(\text{CO})_3(\mathbf{2})]$; the IR data are virtually the same as those reported by van Leeuwen for the oct-1-ene intermediate (Figure 1, 1996, 2019, and 2080 cm^{-1}).⁴⁴ This complex was determined to be the resting state, since upon addition of substrate, it remained as the major rhodium-containing species in solution. In contrast with ligand 1, the rate determining step now appears to be the hydrogenolysis of the acyl complex, liberating the reaction product and forming again the hydride species $[\text{RhH}(\text{CO})_3(\mathbf{2})]$. Remarkably, when the catalytic reaction proceeded, the occurrence of the rhodium hydride was detected, which became the major intermediate at high conversion. Detailed analysis of the concentration profile of rhodium hydride and rhodium acyl in combination with the kinetic studies showed that the hydrogenolysis reaction remained the rate limiting step until full conversion had been obtained. The kinetic profile of the reaction rate was typical of Michaelis–Menten kinetics, and the catalytic reaction rate dependency on the hydrogen concentration showed that the pre-equilibrium toward the metal substrate complex had not been established.⁵²

In a subsequent study, they showed that ligand 1 also induced good selectivity for the linear aldehyde when 2-pentene was the substrate.⁵³ By changing to an analogous benzopinacol derived diphosphite, they obtained 99% selectivity for the linear aldehyde. *In situ* HPIR studies indicated that the highly selective catalyst showed bisequatorial coordination of the diphosphite in the rhodium hydride resting state.

A good example of the usefulness of *in situ* spectroscopy techniques was reported by van Leeuwen and co-workers.⁵⁴ In this article, the research group tested the so-called Buchwald ligands in rhodium-catalyzed hydroformylation (see Figure 9). The catalytic results were comparable to the unmodified rhodium catalyst, and *in situ* spectroscopy measurements were conducted. Surprisingly, it appeared that under the catalytic conditions, the ligands of this class dissociate, forming mainly unmodified $\text{Rh}_6(\text{CO})_{16}$ rather than the more stable $\text{Rh}_4(\text{CO})_{12}$. This is one of the most striking examples of ligand dissociation under hydroformylation conditions.

In 2010, the groups of Matt, Sémeril, and Oberhauser reported the successful use of a calixarene-based bidentate ligand in oct-1-ene hydroformylation.⁵⁵ Linear/branched ratios of up to 16.8 for oct-1-ene and up to 12.4 for styrene were obtained. These very promising ligands were then studied using *in situ* spectroscopic techniques. It appeared that these ligands adopt an *ee* coordination mode in the complex $\mathbf{8 ee}$ - $[\text{RhH}(\text{CO})_2(\text{L})]$ exclusively (Figure 10). This *ee* conformation was already shown to give better regioselectivity in rhodium-catalyzed hydroformylation.⁵⁶

Using similar techniques, the research group of Nozaki reported recently on the activity and stereoselectivity of ligand (*R,S*)-BINAPHOS **9** and its derivatives **10** and **11** in asymmetric hydroformylation (see Figure 11).^{57,58} Unprecedented enantiomeric excesses up to 97.5% were obtained for styrene and up to 89.9% for (*Z*)-2-butene.⁵⁷ To get insight into the reaction mechanism and to identify the active species, *in situ* HPIR and HPNMR spectra were recorded. $^{31}\text{P}\{^1\text{H}\}$ NMR displayed a large coupling constant J_{PH} (160 Hz) accounting for the phosphite center and thus showed its apical orientation, the

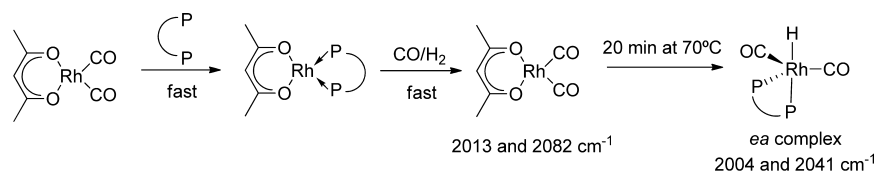


Figure 7. Reactivity of $[\text{Rh}(\text{acac})(\text{CO})_2]$ and **1** with syngas.

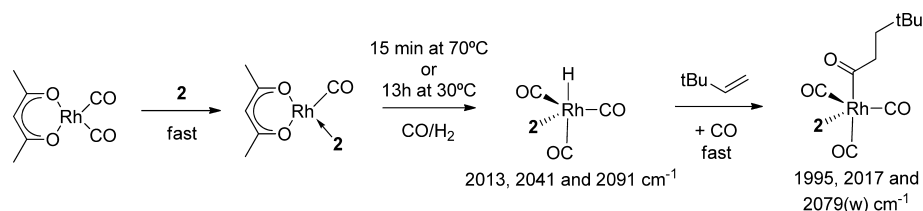


Figure 8. Reactivity of $[\text{Rh}(\text{acac})(\text{CO})_2]$ and **2** with syngas.

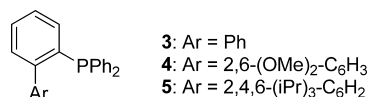


Figure 9. Ligand dissociating from the rhodium center under hydroformylation conditions.

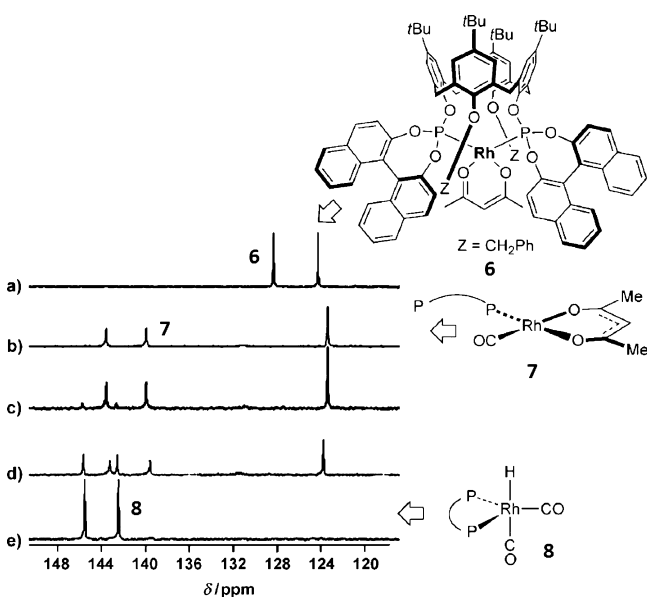


Figure 10. Reactivity of calixarene-modified phosphite rhodium complex **6** under catalytic conditions. $^{31}\text{P}\{^1\text{H}\}$ (a) under argon, (b) under CO (7 bar), (c) under CO/H_2 (1:2 bar 21 bar), r.t., (d) under CO/H_2 (1:2 bar 21 bar), 40 °C, and (e) under CO/H_2 (1:2 bar 21 bar), 50 °C. Reprinted with permission from ref 55. Copyright 2010 Wiley-VCH Verlag GmbH & Co. KGaA.

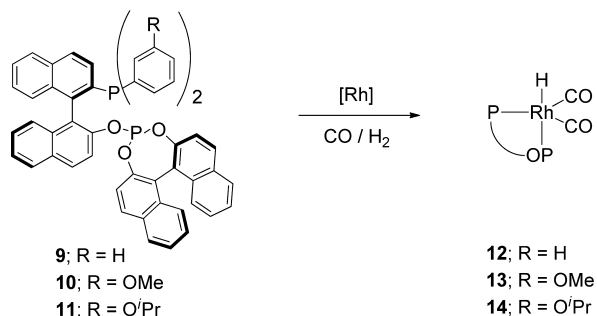


Figure 11. BINAPHOS and derivatives and their reactivity under hydroformylation conditions.

phosphine being in an equatorial position (J_{PH} value of only 23.2 Hz for the phosphine center). ^1H NMR displayed a hydride signal at -8.85 ppm ($J_{\text{RhH}} = 9.8$ Hz). An unidentified species was observed in HPIR ($\nu_{\text{CO}} = 2040$ cm^{-1} , see Figure 12), which disappears with increasing syngas pressure, but

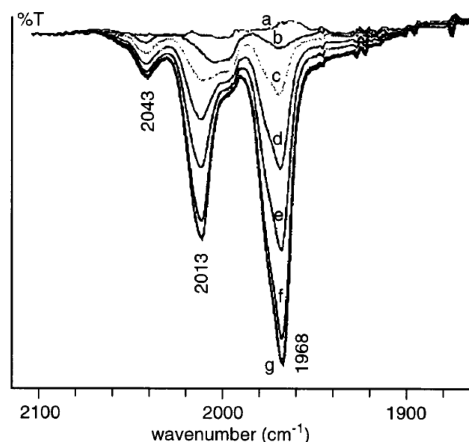


Figure 12. HPIR spectra of OMe-BINAPHOS **10**. Reprinted from ref 59. Copyright 2003 American Chemical Society. Conditions: $[\text{Rh}] = [\text{ligand}] = 50$ mM, $\text{CO}/\text{H}_2 = 40$ bar, 40 °C. (a) $[\text{Rh}(\text{acac})(\text{ligand})]$ without H_2/CO , (b) 0 min with H_2/CO , (c) 12 min, (d) 24 min, (e) 36 min, (f) 48 min, (g) 60–96 min (constant).

clearly the two signals observed at 2014 and 1969 cm^{-1} account for ν_{CO} and ν_{RhH} , respectively (complexes **12**, **13** and **14**, Figure 11).⁵⁹ The observation that the concentration of the unknown species increased with the rhodium concentration and with time during styrene hydroformylation suggested that it concerns a dimeric bridged species, although no bridging CO (at approximately 1800 cm^{-1}) could be detected. It was claimed that this species could be responsible for a decrease in enantioselectivity during the course of the reaction as well at higher rhodium concentration. In a later low temperature NMR and IR study, it was shown that complex **12** does occur as the two *ea* and *ae* isomers, and the one shown in Figure 11 is indeed the major one.⁶⁰ On the basis of the observed $J_{\text{P-H}}$ coupling constants, this was to be anticipated.

The excellent results obtained by Nozaki et al. using nonsymmetrical bidentate ligands prompted several research groups to synthesize new phosphine-phosphite-based ligands. Following up on a systematic study of phosphine-phosphite ligands in hydroformylation⁶¹, van Leeuwen et al. reported new chiral ligands and their use in rhodium-catalyzed asymmetric hydroformylation (Figure 13).⁶² Unfortunately, in this case

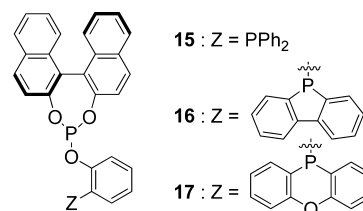


Figure 13. Phosphine-phosphite ligands developed by van Leeuwen et al.

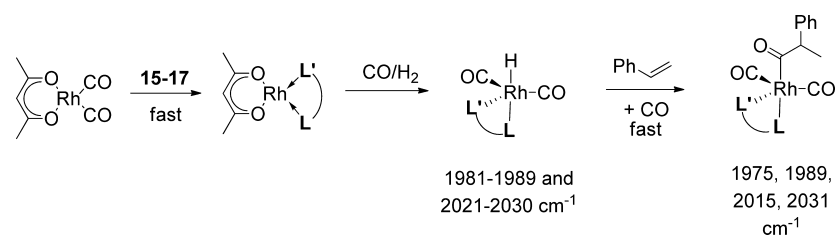


Figure 14. Reactivity of van Leeuwen ligand-modified rhodium species.

enantiomeric excesses did reach up to 55% only using modified styrene substrates. To determine the active species under hydroformylation conditions and to better explain the low enantiodiscrimination, *in situ* spectroscopy techniques were applied and these allowed the detection of different species under hydroformylation conditions. As observed for bulky phosphite **1** (see above), the bidentate ligand (**15**, **16**, and **17**, see Figure 13) reacted with $[\text{Rh}(\text{acac})(\text{CO})_2]$ to form exclusively the complexes $[\text{Rh}(\text{acac})(\text{L})]$, with a *cis* disposition of the donor groups in this case. When syngas pressure was applied, these complexes were transformed into species of the type $[\text{RhH}(\text{CO})_2(\text{L})]$. In these cases, exclusive formation of both *ea* and *ae* type complexes was observed. The addition of styrene resulted in the fast formation of a new rhodium complex, for which the authors postulated *ea* and *ae* acyl species (see Figure 14). It should be noted that the carbonyl of the acyl moiety could not be detected in the infrared spectrum. The absence of absorption bands in the bridging carbonyl section of the HPIR spectrum ruled out the possible formation of carbonyl-bridged bimetallic species.

In 2010, the research group of Reek reported the use of a Taddol-modified INDOLPhos bidentate ligand (see Figure 15)

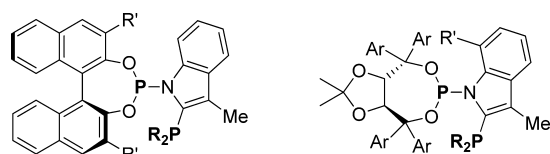


Figure 15. INDOLPhos ligand families reported by Reek. Reprinted from ref 63. Copyright 2010 American Chemical Society.

in rhodium-catalyzed asymmetric hydroformylation.⁶³ This new family of phosphine-phosphite ligands proved to be very effective in the asymmetric hydroformylation of styrene, leading to enantiomeric excesses of up to 72%. Vinyl acetate and allyl cyanide were also suitable substrates for this transformation leading to good ee's. To get insight into the coordination properties of these ligands, HPNMR and HPIR studies were performed. Like in the case of BINAPHOS reported by Nozaki,^{57,59} only *ea* isomers of the complexes $[\text{RhH}(\text{CO})_2(\text{P}-\text{P}^*)]$ were observed, and this observation led the research group to propose a mechanism of enantiodiscrimination, which was also based on DFT calculations.

With the aim to get new rigid ligand backbone structures and wide bite angles, the research group of van Leeuwen developed a new class of ditopic ligands.⁶⁴ The use of hard transition metal linkers afforded assembled bidentate ligands (see Figure 16). The catalytic results in rhodium catalyzed oct-1-ene hydroformylation emphasized the positive effect of the linker; the assembled ligands led to higher regioselectivities than the corresponding nonassembled ditopic ligands. Typically, non-assembled ligands gave *l/b* ratios in the range of 2.8–3.6, whereas the assembled ligand led to *l/b* ratios up to 21. It was thus demonstrated that the hard transition metal linker offers rigidity to the ligand and thus better linearity (calculated bite angle of the range 110–120°). Further to this catalytic experiment, *in situ* spectroscopy was performed under hydroformylation conditions. HPIR experiments showed that the ligand depicted in Figure 16 (bottom right) forms mainly the expected bis-equatorial rhodium dicarbonyl hydride $[\text{RhH}(\text{CO})_2(\text{L})]$ (2044 and 1987 cm^{-1} compared to the equatorial

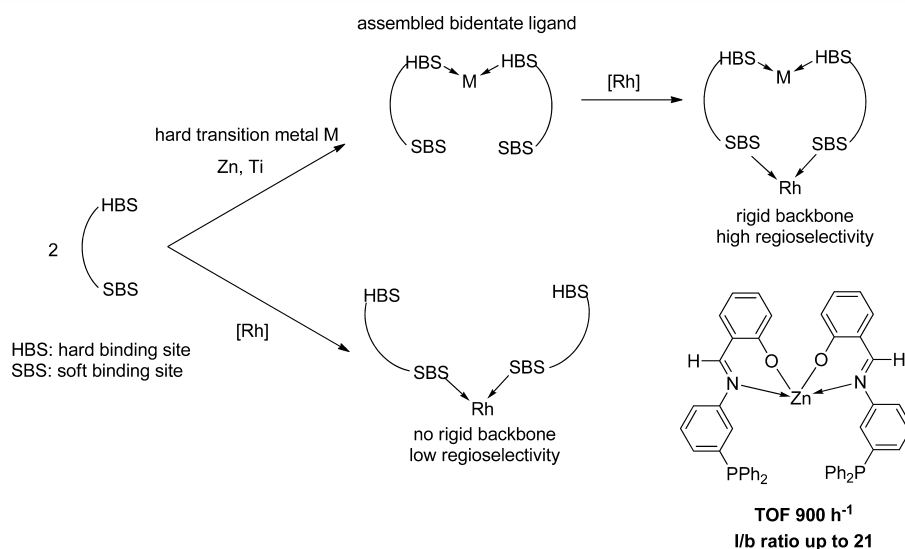


Figure 16. Ditopic ligands and their corresponding early transition metal assemblies.

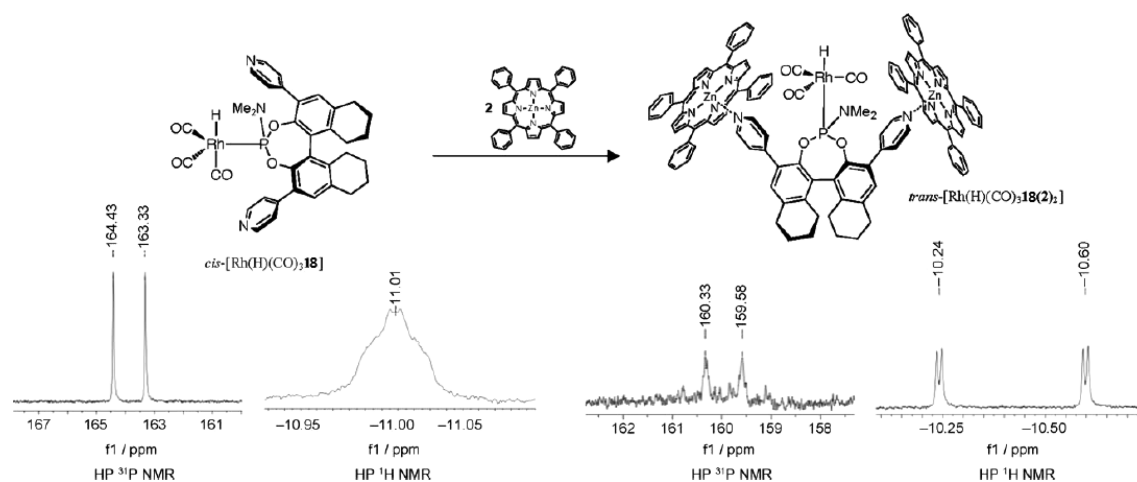


Figure 17. Monoligated complex observed by Reek and co-workers. Reprinted with permission from ref 73. Copyright 2011 Wiley-VCH Verlag GmbH & Co. KGaA.

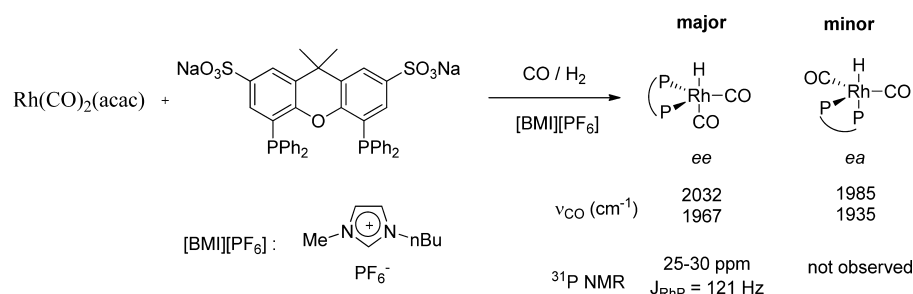


Figure 18. Reactivity of Rh–sulfoxantphos system in ionic liquid under syngas pressure.

apical complex 1987 and 1956 cm^{-1}), known for their higher regiodiscrimination potential.

Reek et al. reported amply during the past decade on the use of templated supramolecular ligands in homogeneous catalysis.^{65–72} In particular, the successful use of these ligands in rhodium-catalyzed asymmetric hydroformylation is of high interest. Recently, a new phosphoramidite-based supramolecular ligand was used in the asymmetric hydroformylation of 2-octene.⁷³ Very high regioselectivities and enantiomeric excesses up to 45% (for 2-methyloctanal) could be achieved. Moreover, these supramolecular assemblies were responsible for higher reaction rates and enantioselectivities. HPNMR studies allowed the determination of the resting state under hydroformylation conditions and it appeared that the monoligated $[\text{RhH}(\text{CO})_3(\mathbf{18})]$ was the main species observed in solution (see Figure 17). According to the authors, the selective formation of a hydride rhodium species in which the supramolecular ligand is in a trans position to the hydride accounts for better enantioselectivity. Indeed it was observed that although the non porphyrin-substituted ligand leads to two different active rhodium hydride isomers, the supramolecular assembled ligand forms a single active species in which the phosphorus atom is trans to the hydride. Although the intermediate alkyl-rhodium and acylrhodium have not been detected, the authors speculate that this preferential coordination mode may be responsible for the improved catalytic results.

3. LIGANDS FOR HYDROFORMYLATION IN IONIC LIQUIDS

The use of ionic liquids (IL) in chemical reactions has been intensively studied during the last decades. As a consequence of

their high boiling point, their low volatility, and their high thermal stability, ionic liquids are potentially suitable for many chemical reactions. Their particular solubilizing and miscibility properties also enable catalytic reactions in biphasic media (IL/organic phase or IL/aqueous phase) where the catalyst is soluble in the ionic liquid phase and can thus be recycled.⁷⁴ For this purpose, new ligands have to be designed for this specific purpose.^{75,76} Sulfoxantphos, the ionic liquid-soluble derivative of Xantphos was used as the ligand for the rhodium-catalyzed hydroformylation in ionic liquids. In 2003, Dupont and van Leeuwen reported an *in situ* study of the formation of rhodium–sulfoxantphos complexes under hydroformylation conditions in ionic liquids.⁷⁷ The two expected active species (*ee* and *ea*) were observed by HPIR in $[\text{BMI}][\text{PF}_6]$, and the phosphorus chemical shift of the major species *ee* could be measured by HPNMR in the same solvent (See Figure 18). The hydride signal could not be observed in ^1H NMR due to intense solvent signals. This report showed the good suitability of this catalytic system since the major compound formed was the one expected to give higher regioselectivities. Nevertheless, it was later observed that certain imidazol(in)ium-based ionic liquids can be deprotonated under the reaction conditions and form interfering transient carbene species.^{78,79} The most active and selective Xantphos based catalyst for IL was reported by Bronger et al.⁸⁰

4. LIGANDS FOR HYDROFORMYLATION IN SUPERCRITICAL CARBON DIOXIDE

Supercritical carbon dioxide (scCO_2) has emerged in the last decades as an interesting alternative for usual organic solvents. Environmentally friendly, cheap, highly compressible, highly

miscible with gases and easily reusable, scCO_2 has interested many chemists, from academia and industry. Many efforts were made to improve catalytic performance. scCO_2 is a nonpolar solvent, but often ligand modifications are required to increase the solubility of the catalyst systems. The introduction of perfluoroalkyl chains was successful academically,^{81–83} but the difficulty of their synthesis and their cost remain a major drawback for industrial applications. The introduction of long alkyl chains on the ligands can have dramatic influences on the solubility of the ligand,⁸⁴ and to this end Masdeu-Bultó et al. reported the synthesis of ligands $\text{PPh}_x(\text{O}-\text{C}_9\text{H}_{19})_{3-x}$ where the alkyl chain is branched (see Figure 19, left).⁸⁵ Unfortunately,

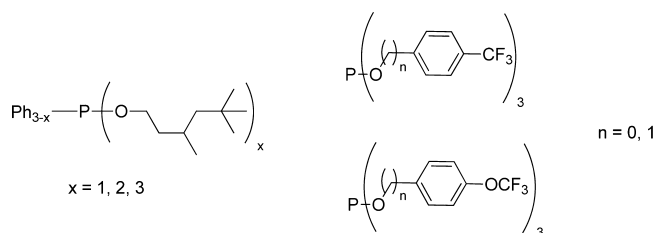


Figure 19. Potential scCO_2 -soluble ligands developed by Masdeu-Bultó et al.

the corresponding rhodium complexes were poorly soluble in scCO_2 , and thus the hydroformylation activities could not outperform the ones observed for the same ligands in toluene. However, the research group performed HPNMR and HPIR experiments in toluene to get more insight into this catalytic system. Many different complexes could be detected such as $[\text{RhH}(\text{L})_4]$, $[\text{RhH}(\text{CO})(\text{L})_3]$, and $[\text{RhH}(\text{CO})_2(\text{L})_2]$ with ^{31}P and ^1H NMR, and the stretching vibration frequencies of the carbonyl groups could be successfully assigned.

Following the same strategy, the same group published a few years later a similar study using scCO_2 -soluble trifluoromethyl-substituted phosphites (see Figure 19, right).⁸⁶ Under hydroformylation conditions in methyltetrahydrofuran, complexes of the type $[\text{RhH}(\text{CO})(\text{L})_3]$ and $[\text{RhH}(\text{L})_4]$ were detected by HPIR and HPNMR (^1H and ^{31}P), giving similar reactivity as triphenyl phosphite-modified rhodium systems.

5. HYDROAMINOMETHYLATION

During the last decades, cascade reactions involving a hydroformylation step have found increasing interest. The major product aldehyde is often not the target for applications as they are usually further oxidized, reduced, or coupled to form added-value products. With this in mind, many cascade reactions were developed,⁸⁷ including hydroformylation-hydrogenation,^{88–93} hydroformylation-cyclization,^{94–96} isomerization-hydroformylation,^{97–103} hydroformylation-acetalization,^{104,105} and the well-known hydroaminomethylation (HAM),^{106–108} the latter consisting of a cascade hydroformylation-reductive amination. The full mechanism of the HAM reaction has not been proven yet, and the real active species have not been unambiguously identified. It is even

suspected that two different active species accounting for each reaction sequence are present in solution.¹⁰⁶ Van Leeuwen, Beller, and co-workers reported in 2006 an *in situ* study in order to determine reaction pathways or some reaction intermediates.¹⁰⁹ In this case, the substrate used was 2-pentene, so the overall reaction can be seen as an isomerization-hydroformylation-reductive amination cascade (see Figure 20).¹¹⁰

6. TANDEM HYDROFORMYLATION-HYDROGENATION REACTION

In 2009, the research group of Breit reported a very efficient catalytic system for the direct production of linear alcohols from terminal alkenes by tandem hydroformylation-hydrogenation.⁹¹ In 2012, the use of a cooperative ligand system was reported for the same transformation (in a similar approach as Cole-Hamilton and co-workers with Xantphos and triethylphosphine).⁸⁸ It was supposed that two different active species were formed under the catalytic conditions, each one providing fast and selective transformations. Tuning the electronic properties of each ligand, and by these adjusting activities and equilibrium constants between the different active species, allowed getting unprecedented chemo- and regioselectivities.¹¹¹ To identify each species and understand their catalytic role, the catalytic system was studied by HPIR under the reaction conditions. Various species could be identified (see Figure 21), and kinetic studies could assign the activity and selectivity of the formed species in each transformation.

7. ALKOXYCARBONYLATION

Alkoxy carbonylation, usually methoxycarbonylation, is a very efficient method to produce esters from readily available alkene and alkyne feedstocks. Similar to hydroformylation, this reaction involves the formation of a carbon–carbon bond by addition of a molecule of carbon monoxide. Initially, this reaction was catalyzed by modified cobalt catalyst precursors and has been extensively studied by various chemical companies. In 1982, Milstein et al. reported a mechanistic study showing the high activity of intermediates of the type $[\text{RO}-\text{C}(\text{=O})-\text{Co}(\text{CO})_x(\text{L})_{4-x}]$ that are believed to be the active species in this case.¹¹² Indeed, such species readily react with olefins, losing a carbon monoxide molecule.

The formation of dimethyl adipate from a double methoxycarbonylation of butadiene is a very promising reaction, since the formation of adipic acid is highly desirable for the production of nylon 66 (Figure 22). A three-step process, producing adipic acid, using modified cobalt catalysts was investigated at BASF and tested in a pilot plant.¹¹³ Another process producing adipic acid from butadiene was studied by DuPont.¹¹⁴ In 2002, the research group of Beller reported the methoxycarbonylation of 1,3-butadiene using a dppb-modified palladium catalyst.¹¹⁵

The complete mechanism of cobalt-catalyzed methoxycarbonylation of butadiene was the topic of a very interesting report by the research group of Horváth.¹¹⁶ HPIR and HPNMR

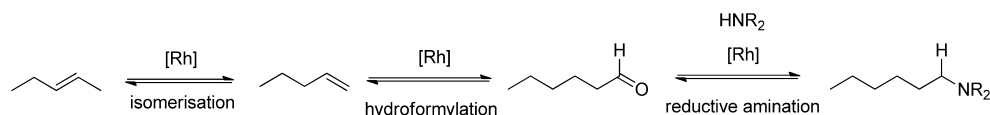


Figure 20. Hydroaminomethylation of 2-pentene.

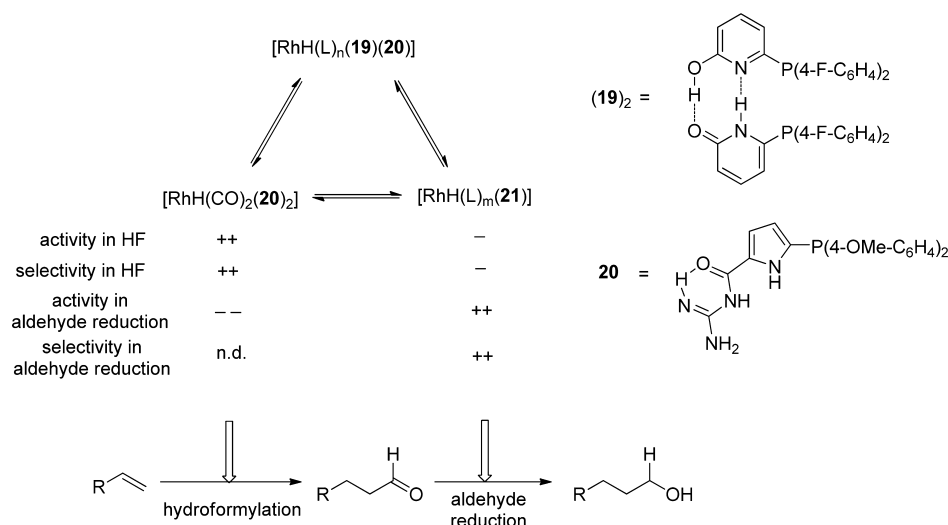


Figure 21. Cooperative ligand system for selective formation of linear alcohols from terminal alkenes.

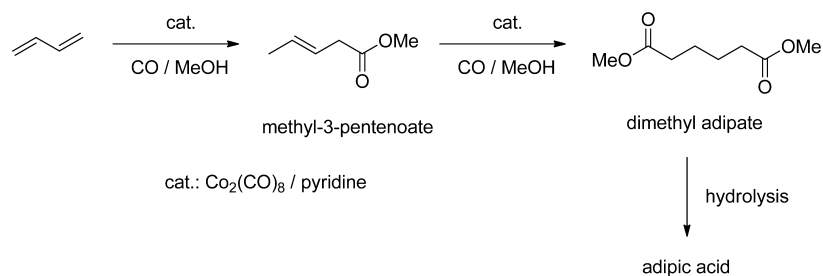


Figure 22. Methoxycarbonylation of butadiene.

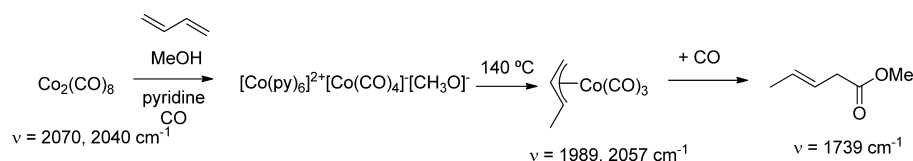


Figure 23. Reaction of cobalt carbonyl cluster under methoxycarbonylation conditions.

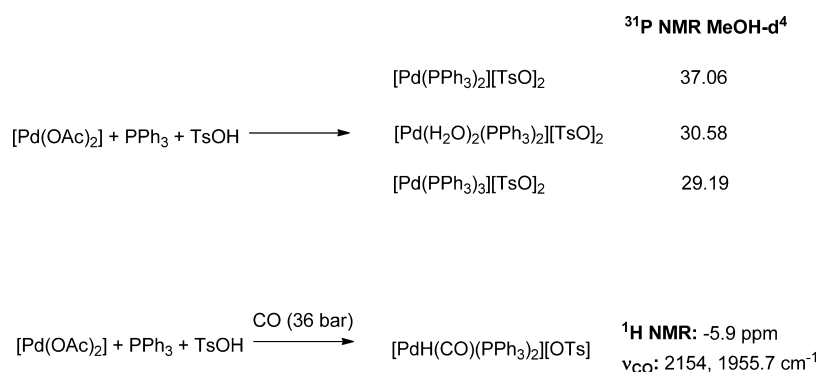


Figure 24. Formation of cationic palladium species under catalytic conditions.

studies of the methoxycarbonylation of 1,3-butadiene to methyl-3-pentenoate in methanol in the presence of [Co₂(CO)₈] and pyridine under carbon monoxide led to a good understanding of the reaction mechanism. It was shown that under catalytic conditions, the salt [Co(py)₆][Co(CO)₄][OCH₃] was the main cobalt-containing species in solution. Heating the reaction to 140 °C in the presence of 1,3-butadiene allowed the formation of the η^3 -crotyl cobalt complex,

eventually forming methyl-3-pentenoate (Figure 23). Using variable temperature HPIR techniques, many reaction intermediates could be detected.

The methoxycarbonylation of other substrates than 1,3-butadiene was also investigated. As an example, Chaudhari and co-workers studied the methoxycarbonylation of styrene using a modified-palladium catalyst. HPNMR studies under a carbon monoxide pressure allowed the detection of different species in

solution (see Figure 24).¹¹⁷ Other reaction intermediates could also be observed, mainly as decomposition products of the species depicted in Figure 24. It was shown that the formation of carbomethoxy palladium species "Pd-C(=O)OMe" is very unlikely in acidic media. The hydride palladium complex [PdH(CO)(PPh₃)₂][OTs] was strongly suggested to be the active species in this reaction that initiates the catalytic cycle. The formation of this hydride complex under acidic conditions explains the enhanced reaction rate observed when the methoxycarbonylation is conducted in the presence of TsOH (TOF increased from 52 to 221 h⁻¹).¹¹⁷

Important to note is the *in situ* analysis of the metallic complexes formed when the substrate styrene is added (see Figure 25). Both iso- and linear alkyl palladium complexes were

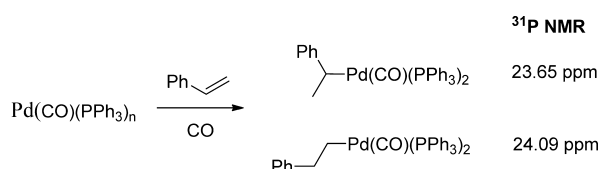


Figure 25. Formation of alkylpalladium species under catalytic conditions.

observed. Importantly, no acyl palladium intermediates were detected pointing out the rate limiting carbonyl insertion in this case.

This report is a very good example of the possibilities that *in situ* spectroscopy offers for the determination of reaction intermediates and the active species and for a better understanding of the catalytic cycle. Moreover, these techniques open doors for further catalytic improvements.

In 1999, the research groups of Heaton, Iggo, and Whyman reported the use of modified palladium and platinum catalysts for the methoxycarbonylation of ethylene to methyl propanoate.^{118,119} *In situ* HPNMR experiments allowed for good understanding of the reaction.¹²⁰ In particular, all intermediates involved in the platinum catalyzed reaction could be identified. The poisoning effect of carbon monoxide could also be identified as cause for the low activity of platinum catalysts compared to palladium-based catalysts (see Figure 26).

More recently, Eastham, Iggo, and Claver et al. reported on the *in situ* HPNMR study of palladium catalyzed methoxycarbonylation of ethene.¹²¹ Using a class of bulky, strongly σ -donating bidentate ligands with different backbones, several reaction intermediates could be detected (see Figure 27). In particular, tris-coordinated [Pd(CH₂CH₃)(P-P)]⁺, resulting from the ethylene insertion in the Pd-hydride bond, could be detected and the observed NMR data were compared to simulated spectra at variable temperature. Figure 28 shows the particular example of complex [Pd(Et)(24)]⁺ that exists in the form of two conformers in solution at 193 K. This was

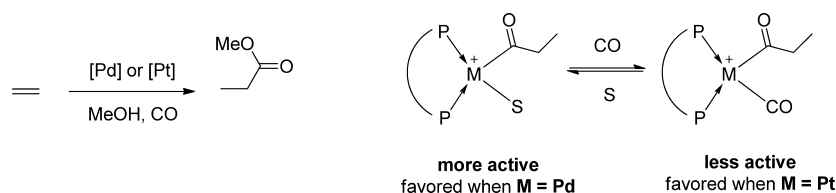


Figure 26. Detection of reaction intermediates in ethylene methoxycarbonylation.

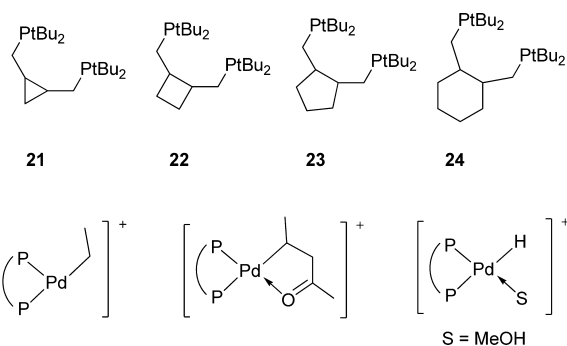


Figure 27. Ligands used and the organometallic species detected.

explained by a rapid insertion-desinsertion fluxional process where the two phosphorus centers remain distinct.

8. PALLADIUM CATALYZED STYRENE/CO COPOLYMERIZATION

Another interesting example of a homogeneously catalyzed reaction involving CO is the alkene-CO copolymerization. Palladium catalyzed styrene-CO copolymerization has been widely studied using nitrogen-based ligands. Indeed, phosphorus based ligands can favor beta-hydride elimination, leading to shorter chain length and the formation of less active Pd-benzyl species. Nevertheless, phosphorus-based ligand for this purpose could allow the use of *in situ* techniques and thus of a better understanding of the reaction. The research groups of Nozaki, Matsubara, and Koga reported in 1997 the exceptional activity of (*R,S*)-BINAPHOS ligand **9** for the isotactic copolymerization of alkenes (styrene or propene) and carbon monoxide.^{122,123} High-pressure NMR studies of the styrene-CO copolymerization using this system was reported in 2003 by the groups of Iggo and Nozaki.¹²⁴ This powerful tool allowed them to detect several reaction intermediates and to propose the catalytic pathway (see Figure 29). It was observed that styrene gave preferably 1,2 insertion to form intermediate **26** instead of **27**. CO insertion follows forming **28** and **29**, which could be detected in ³¹P{¹H} NMR, allowing the chain to grow. Polymer liberation, occurring via β -hydride elimination, is much slower than additional styrene insertion leading to high molecular weight polymers (up to 104 400 g mol⁻¹). Interestingly, again in this example, crucial insight into the reaction mechanism could be obtained using these powerful techniques.

9. CONCLUSIONS

In conclusion, the development of powerful *in situ* spectroscopic techniques has contributed greatly to in-depth understanding of catalytic reactions under real process conditions. Especially a fast *in situ* IR autoclave is extremely suited to study fast catalytic reactions such as the rhodium catalyzed hydroformylation. Intimate mechanistic information can be obtained by rapid scan techniques, even for very fast reactions at very low

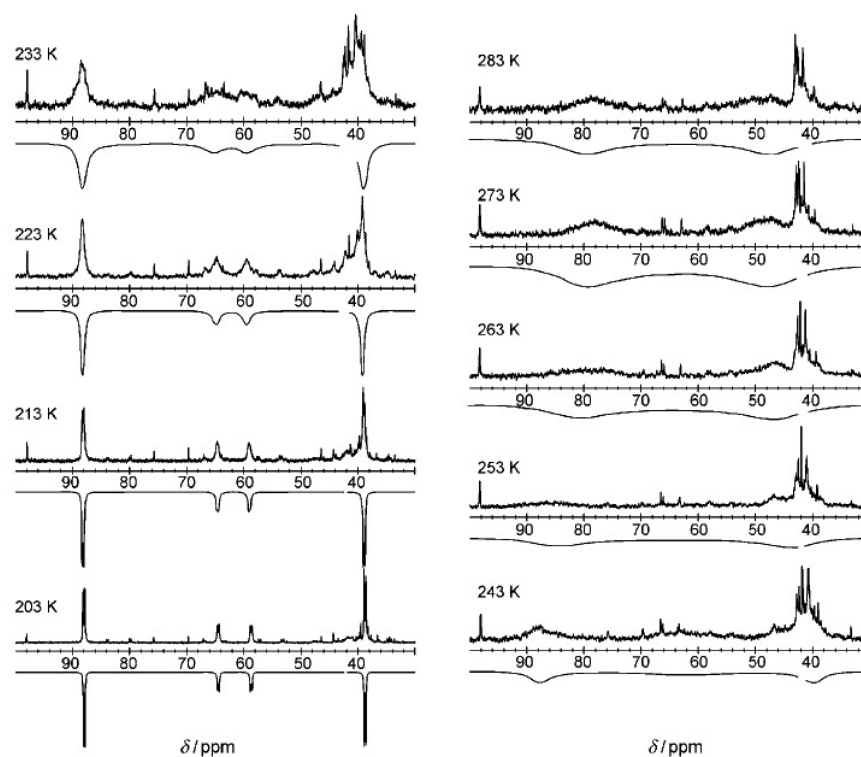


Figure 28. $^{31}\text{P}\{^1\text{H}\}$ spectra and simulation at VT of $[\text{Pd}(\text{CH}_2\text{CH}_3)(\mathbf{24})]$. Complex formation conditions: $[\text{Pd}(\text{O}_2\text{CCF}_3)(\mathbf{23})]$ with excess trifluoroacetic acid in methanol under 10 bar of ethylene at 353 K for 20 min. Reprinted with permission from ref 121. Copyright 2010 Wiley-VCH Verlag GmbH & Co. KGaA.

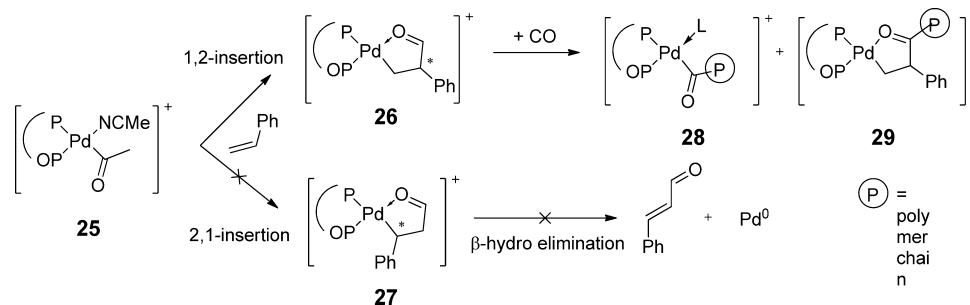


Figure 29. Catalytic pathway proposed by Nozaki et al. for the Pd-BINAPHOS-catalyzed copolymerization of styrene and CO.

concentrations and catalytic conditions. More detailed structural information can be obtained by high pressure NMR studies, which nowadays can also be performed without mass transfer limitation using flow conditions. The lower sensitivity of NMR compared to IR does require higher concentrations than usually used in catalytic systems. Nevertheless, the combination of these techniques has already contributed to solving the mechanisms of several important catalytic reactions.

Rational ligand design for obtaining new or improved catalyst structures is still a tremendously challenging task, and admittedly most powerful catalysts have been discovered merely by trial and error. Most catalytic cycles are a complex sequence of elementary reaction steps with many possible side- and derailment reactions. Changes in catalyst structure can be expected to influence many of them. The power of real operando spectroscopic techniques such as HP-NMR and IR discussed in this review provide intimate insight in the mechanistic details of the catalytic reaction. Once detailed knowledge of the exact nature of important parts of the

catalytic reaction as rate- and/or selectivity-determining steps and nature of catalyst derailment and decomposition pathways have been identified, real rational catalyst design will become within reach.

AUTHOR INFORMATION

Corresponding Author

*E-mail: pcjk@st-andrews.ac.uk.

Notes

The authors declare no competing financial interest.

REFERENCES

- (1) Young, J. F.; Osborn, J. A.; Jardine, F. A.; Wilkinson, G. J. *Chem. Soc., Chem. Commun.* **1965**, 131.
- (2) Tolman, C. A. *J. Am. Chem. Soc.* **1970**, *92*, 2953.
- (3) Drago, R. S.; Joerg, S. *J. Am. Chem. Soc.* **1996**, *118*, 2654.
- (4) Joerg, S.; Drago, R. S.; Sales, J. *Organometallics* **1998**, *17*, 589.
- (5) Golovin, M. N.; Rahman, M. M.; Belmonte, J. E.; Giering, W. P. *Organometallics* **1985**, *4*, 1981.

- (6) Fernandez, A.; Wilson, M. R.; Woska, D. C.; Prock, A.; Giering, W. P.; Haar, C. M.; Nolan, S. P.; Foxman, B. M. *Organometallics* **2002**, *21*, 2758.
- (7) Tolman, C. A. *Chem. Rev.* **1977**, *77*, 313.
- (8) White, D.; Tavener, B. C.; Coville, N. J.; Wade, P. W. J. *Organomet. Chem.* **1995**, *495*, 41.
- (9) Brown, T. L. *Inorg. Chem.* **1992**, *31*, 1286.
- (10) Koide, Y.; Bott, S. G.; Barron, A. R. *Organometallics* **1996**, *15*, 2213.
- (11) Angermund, K.; Baumann, W.; Dinjus, E.; Fornika, R.; Goerls, H.; Kessler, M.; Krueger, C.; Leitner, W.; Lutz, F. *Chem.—Eur. J.* **1997**, *3*, 755.
- (12) Clavier, H.; Nolan, S. P. *Chem. Commun.* **2010**, *46*, 841.
- (13) Hillier, A. C.; Sommer, W. J.; Yong, B. S.; Petersen, J. L.; Cavallo, L.; Nolan, S. P. *Organometallics* **2003**, *22*, 4322.
- (14) Poater, A.; Cosenza, B.; Correa, A.; Giudice, S.; Ragone, F.; Scarano, V.; Cavallo, L. *Eur. J. Inorg. Chem.* **2009**, 1759.
- (15) Thorn, D. L.; Hoffmann, R. J. *Am. Chem. Soc.* **1978**, *100*, 2079.
- (16) Dekker, G. P. C. M.; Elsevier, C. J.; Vrieze, K.; van Leeuwen, P. W. N. M. *J. Organomet. Chem.* **1992**, *430*, 357.
- (17) Casey, C. P.; Whiteker, G. T. *Isr. J. Chem.* **1990**, *30*, 299.
- (18) Kamer, P. C. J.; van Leeuwen, P. W. N. M.; Reek, J. N. H. *Acc. Chem. Res.* **2001**, *34*, 895.
- (19) Gillespie, J. A.; Dodds, D. L.; Kamer, P. C. J. *Dalton Trans.* **2010**, *39*, 2751.
- (20) *Mechanisms in Homogeneous Catalysis: A Spectroscopic Approach*; Heaton, B., Ed.; Wiley VCH: Weinheim, Germany, 2005.
- (21) For a previous review on the topic, see Kamer, P. C. J.; van Rooy, A.; Schoemaker, G. C.; van Leeuwen, P. W. N. M. *Coord. Chem. Rev.* **2004**, *248*, 2409.
- (22) Roe, D. C. J. *Magn. Reson.* **1985**, *63*, 388.
- (23) Horvath, I. *Organometallics* **1986**, *5*, 2333.
- (24) Roe, D. E. *Organometallics* **1987**, *6*, 942.
- (25) Horvath, I. T.; Kiss, G.; Cook, R. A.; Bond, J. E.; Stevens, P. A.; Rábai, J.; Mozeleski, E. J. *J. Am. Chem. Soc.* **1998**, *120*, 3133.
- (26) Gaemers, S.; Luyten, H.; Ernsting, J. M.; Elsevier, C. J. *Magn. Reson. Chem.* **1999**, *37*, 25.
- (27) Wittmann, K.; Wisniewski, W.; Mynott, R.; Leitner, W.; Kranemann, C. L.; Rische, T.; Eilbracht, P.; Gaemers, S.; Ernsting, J. M.; Elsevier, C. J. *Chem.—Eur. J.* **2001**, *7*, 4584.
- (28) Kuhn, L. T.; Bargon, J. *Top. Curr. Chem.* **2007**, *276*, 25.
- (29) Duckett, S. B.; Blazina, D. *Eur. J. Inorg. Chem.* **2003**, 2901.
- (30) Duckett, S. B.; Mewis, R. B. *Acc. Chem. Res.* **2012**, *45*, 1247.
- (31) Iggo, J. A.; Shirley, D.; Tong, N. C. *New J. Chem.* **1998**, 1043.
- (32) Selent, D.; Baumann, W.; Boerner, A. Gas Introduction and Circulation Apparatus for Monitoring Reactions in the Liquid Phase under Participation of Gaseous Reactants under Normal and High Pressure by Means of Nuclear Resonance Spectroscopy (pressure NMR spectroscopy) under Stationary Conditions. German patent DE 10333143, July 17, 2005; Chem. Abstr. CAN142:263666.
- (33) Noack, K. *Spectrochim. Acta* **1968**, *24A*, 1917.
- (34) Moser, W. R.; Cnossen, J. E.; Wang, A. W.; Krouse, S. A. *J. Catal.* **1985**, *95*, 21.
- (35) Moser, W. R.; Papile, C. J.; Brannon, D. A.; Duwell, R. A. *J. Mol. Catal.* **1987**, *41*, 271.
- (36) Rigby, W.; Whyman, R.; Wilding, K. J. *Phys. E: Sci. Instrum.* **1970**, *3*, 572.
- (37) Whyman, R.; Hunt, K. A.; Page, R. W.; Rigby, W. J. *Phys. E: Sci. Instrum.* **1984**, *17*, 559.
- (38) Whyman, R. *J. Organomet. Chem.* **1974**, *66*, C23.
- (39) Chew, W.; Widjaja, E.; Garland, M. *Organometallics* **2002**, *21*, 1982.
- (40) Widjaja, E.; Li, C.; Garland, M. *Organometallics* **2002**, *21*, 1991.
- (41) Li, C.; Widjaja, E.; Garland, M. *J. Am. Chem. Soc.* **2002**, *125*, 5540.
- (42) Li, C.; Chen, L.; Garland, M. *J. Am. Chem. Soc.* **2007**, *129*, 13327.
- (43) Li, C.; Chen, L.; Garland, M. *Adv. Synth. Catal.* **2008**, *350*, 679.
- (44) Van Rooy, A.; Oriij, E.; Kamer, P. C. J.; Van Leeuwen, P. W. N. M. *Organometallics* **1995**, *14*, 34.
- (45) Jongsmá, T.; Challa, G.; Van Leeuwen, P. W. N. M. *J. Organomet. Chem.* **1991**, *421*, 121.
- (46) Crous, R.; Datt, M.; Foster, D.; Bennie, L.; Steenkamp, C.; Huysen, J.; Kirsten, L.; Steyl, G.; Roodt, A. *Dalton Trans.* **2005**, 1108.
- (47) van der Slot, S. C.; Kamer, P. C. J.; van Leeuwen, P. W. N. M.; Iggo, J. A.; Heaton, B. T. *Organometallics* **2001**, *20*, 430.
- (48) van der Slot, S. C.; Kamer, P. C. J.; van Leeuwen, P. W. N. M.; Fraanje, J.; Goubitz, K.; Lutz, M.; Spek, A. L. *Organometallics* **2000**, *19*, 2504.
- (49) van der Veen, L. A.; Kamer, P. C. J.; van Leeuwen, P. W. N. M. *Organometallics* **1999**, *18*, 4765.
- (50) Walczuk, E.; Kamer, P. C. J.; van Leeuwen, P. W. N. M. *Angew. Chem., Int. Ed.* **2003**, *42*, 4665.
- (51) Kubis, C.; Ludwig, R.; Sawall, M.; Neymeyr, K.; Börner, A.; Wiese, K.-D.; Hess, D.; Franke, R.; Selent, D. *ChemCatChem* **2010**, *2*, 287.
- (52) Kubis, C.; Selent, D.; Sawall, M.; Ludwig, R.; Neymeyr, K.; Baumann, W.; Franke, R.; Börner, A. *ChemCatChem* **2010**, *2*, 287.
- (53) Selent, D.; Franke, R.; Kubis, C.; Spannenberg, A.; Baumann, W.; Kreidler, B.; Börner, A. *Organometallics* **2011**, *30*, 4509.
- (54) Rafter, E.; Gilheany, D. G.; Reek, J. N. H.; van Leeuwen, P. W. N. M. *ChemCatChem* **2010**, *2*, 387.
- (55) Sémeril, D.; Matt, D.; Toupet, L.; Oberhauser, W.; Bianchini, C. *Chem.—Eur. J.* **2010**, *16*, 13843.
- (56) van Leeuwen, P. W. N. M.; Kamer, P. C. J.; Reek, J. N. H.; Dierkes, P. *Chem. Rev.* **2000**, *100*, 2741.
- (57) Nozaki, K.; Sakai, N.; Nanno, T.; Higashijima, T.; Mano, S.; Horiuchi, T.; Takaya, H. *J. Am. Chem. Soc.* **1997**, *119*, 4413.
- (58) Nozaki, K.; Matsuo, T.; Shibahara, F.; Hiyaman, T. *Adv. Synth. Catal.* **2001**, *343*, 61.
- (59) Nozaki, K.; Matsuo, T.; Shibahara, F.; Hiyama, T. *Organometallics* **2003**, *22*, 594.
- (60) Castillo Molina, D. A.; Casey, C. P.; Mueller, I.; Nozaki, K.; Jaekel, C. *Organometallics* **2010**, *29*, 3362.
- (61) Deerenberg, S.; Kamer, P. C. J.; Van Leeuwen, P. W. N. M. *Organometallics* **2000**, *19*, 2065.
- (62) Doro, F.; Reek, J. N. H.; van Leeuwen, P. W. N. M. *Organometallics* **2010**, *29*, 4440.
- (63) Wassenaar, J.; de Bruin, B.; Reek, J. N. H. *Organometallics* **2010**, *29*, 2767.
- (64) Rivillo, D.; Gulyás, H.; Benet-Buchholz, J.; Escudero-Adán, E. C.; Freixa, Z.; van Leeuwen, P. W. N. M. *Angew. Chem., Int. Ed.* **2007**, *46*, 7247.
- (65) Slagt, V. F.; van Leeuwen, P. W. N. M.; Reek, J. N. H. *Dalton Trans.* **2007**, 2302.
- (66) Kuil, M.; Goudriaan, P. E.; Kleij, A. W.; Tooke, D. M.; Spek, A. L.; van Leeuwen, P. W. N. M.; Reek, J. N. H. *Dalton Trans.* **2007**, 2311.
- (67) Goudriaan, P. E.; Jang, X.-B.; Kuil, A.; Lemmens, R.; van Leeuwen, P. W. N. M.; Reek, J. N. H. *Eur. J. Org. Chem.* **2008**, 6079.
- (68) Kuil, M.; Goudriaan, P. E.; van Leeuwen, P. W. N. M.; Reek, J. N. H. *Chem. Commun.* **2006**, 4679.
- (69) Reek, J. N. H.; Röder, M.; Goudriaan, P. E.; Kamer, P. C. J.; van Leeuwen, P. W. N. M.; Slagt, V. F. *J. Organomet. Chem.* **2005**, *690*, 4505.
- (70) Slagt, V. F.; Reek, J. N. H.; Kamer, P. C. J.; van Leeuwen, P. W. N. M. *Angew. Chem., Int. Ed.* **2001**, *40*, 4271.
- (71) Slagt, V. F.; Kamer, P. C. J.; van Leeuwen, P. W. N. M.; Reek, J. N. H. *J. Am. Chem. Soc.* **2004**, *126*, 1526.
- (72) Slagt, V.; Röder, M.; Kamer, P. C. J.; van Leeuwen, P. W. N. M.; Reek, J. N. H. *J. Am. Chem. Soc.* **2004**, *126*, 4056.
- (73) Bellini, R.; Chikkali, S. H.; Berthon-Gelloz, G.; Reek, J. N. H. *Angew. Chem., Int. Ed.* **2011**, *50*, 7342.
- (74) For a review on hydroformylation in ionic liquids, see Haumann, M.; Riisager, A. *Chem. Rev.* **2008**, *108*, 1474.
- (75) Chauvin, Y.; Mussmann, L.; Olivier, H. *Angew. Chem., Int. Ed.* **1995**, *34*, 3698.

- (76) Kong, F.; Jiang, J.; Jin, Z. *Catal. Lett.* **2004**, *96*, 63.
- (77) Silva, S. M.; Bronger, R. P. J.; Freixa, Z.; Dupont, J.; van Leeuwen, P. W. N. M. *New. J. Chem.* **2003**, *27*, 1294.
- (78) Scholten, J. D.; Dupont, J. *Organometallics* **2008**, *27*, 4439.
- (79) This effect was also observed in hydroaminomethylation: Hamers, B.; Bäuerlein, P.; Müller, C.; Vogt, D. *Adv. Synth. Catal.* **2008**, *350*, 332.
- (80) Bronger, R. P. J.; Silva, S. M.; Kamer, P. C. J.; van Leeuwen, P. W. N. M. *Dalton Trans.* **2004**, 1590.
- (81) Koch, D.; Leitner, W. *J. Am. Chem. Soc.* **1998**, *120*, 13398.
- (82) Banet Osuna, A. M.; Chen, W.; Hope, E. G.; Kemmitt, R. D. W.; Paige, D. R.; Stuart, A. M.; Xiao, J.; Xu, L. *J. Chem. Soc., Dalton Trans.* **2000**, 4052.
- (83) Sellin, M. F.; Bach, I.; Webster, J. M.; Montilla, F.; Rosa, V.; Avilés, T.; Poliakkoff, M.; Cole-Hamilton, D. J. *J. Chem. Soc., Dalton Trans.* **2002**, 4569.
- (84) Bach, I.; Cole-Hamilton, D. J. *Chem. Commun.* **1998**, 1463.
- (85) Giménez-Pedros, M.; Aghmiz, A.; Ruiz, N.; Masdeu-Bultó, A. M. *Eur. J. Inorg. Chem.* **2006**, 1067.
- (86) Estorach, C. T.; Orejón, A.; Masdeu-Bultó, A. M. *Green Chem.* **2008**, *10*, 545.
- (87) Eilbracht, P.; Bäracker, L.; Buss, C.; Hollmann, C.; Kitsos-Ryzchon, B. E.; Kranenmann, C. L.; Rische, T.; Roggenbuck, R.; Schmidt, A. *Chem. Rev.* **1999**, *99*, 3329.
- (88) McDougall, J. K.; Simpson, M. C.; Green, M. J.; Cole-Hamilton, D. J. *J. Chem. Soc., Dalton Trans.* **1996**, 1161.
- (89) Cheliatsidou, P.; White, D. F. S.; Cole-Hamilton, D. J. *Dalton Trans.* **2004**, 3425.
- (90) Boogaerts, I. I. F.; White, D. F. S.; Cole-Hamilton, D. J. *Chem. Commun.* **2010**, 46, 2194.
- (91) Diab, L.; Šmejkal, T.; Geier, J.; Breit, B. *Angew. Chem., Int. Ed.* **2009**, *48*, 8022.
- (92) Takahashi, K.; Yamashita, M.; Ichihara, T.; Makano, K.; Nozaki, K. *Angew. Chem., Int. Ed.* **2011**, *49*, 1.
- (93) Diebolt, O.; Müller, C.; Vogt, D. *Catal. Sci. Technol.* **2012**, *2*, 773.
- (94) Eilbracht, P.; Schmidt, A. M. *Top. Organomet. Chem.* **2006**, *18*, 65 and references therein.
- (95) Breit, B. *Angew. Chem., Int. Ed.* **1996**, *35*, 2835.
- (96) Bäuerlein, P. S.; Arenas Gonzalez, I.; Weemers, J. J. M.; Lutz, M.; Spek, A. L.; Vogt, D.; Müller, C. *Chem. Commun.* **2009**, 4944.
- (97) van der Veen, L. A.; Kamer, P. C. J.; van Leeuwen, P. W. N. M. *Angew. Chem., Int. Ed.* **1999**, *38*, 336.
- (98) Selent, D.; Hess, D.; Wiese, K.-D.; Röttger, D.; Kunze, C.; Börner, A. *Angew. Chem., Int. Ed.* **2001**, *40*, 1696.
- (99) Klein, H.; Jackstell, R.; Wiese, K.-D.; Borgmann, C.; Beller, M. *Angew. Chem., Int. Ed.* **2001**, *40*, 3408.
- (100) Behr, A.; Obst, D.; Schulte, C.; Schosser, T. *J. Mol. Catal. A: Chem.* **2003**, *206*, 179.
- (101) Yan, Y.; Zhang, X.; Zhang, X. *J. Am. Chem. Soc.* **2006**, *128*, 16058.
- (102) Sémeril, D.; Jeunesse, C.; Matt, D.; Toupet, L. *Angew. Chem., Int. Ed.* **2006**, *45*, 5810.
- (103) Janssen, M.; Bini, L.; Hamers, B.; Müller, C.; Hess, D.; Christiansen, A.; Pranke, R.; Vogt, D. *Adv. Synth. Catal.* **2010**, *51*, 1971.
- (104) Beller, M.; Cornils, B.; Frohning, C. D.; Kohlpainter, C. W. *J. Mol. Catal. A* **1995**, *104*, 17.
- (105) Diebolt, O.; Cruzeuil, C.; Müller, C.; Vogt, D. *Adv. Synth. Catal.* **2012**, *354*, 670.
- (106) Zimmermann, B.; Herwig, J.; Beller, M. *Angew. Chem., Int. Ed.* **1999**, *111*, 2515.
- (107) Ahmed, M.; Seayad, A. M.; Jackstell, R.; Beller, M. *J. Am. Chem. Soc.* **2003**, *125*, 10311.
- (108) Hamers, B.; Koscuisko-Morizet, E.; Müller, C.; Vogt, D. *ChemCatChem* **2009**, *1*, 103.
- (109) Ahmed, M.; Bronger, R. P. J.; Jackstell, R.; Kamer, P. C. J.; van Leeuwen, P. W. N. M.; Beller, M. *Chem.—Eur. J.* **2006**, *12*, 8979.
- (110) Such reaction sequences were already reported: Seayad, A.; Ahmed, M.; Klein, H.; Jackstell, R.; Gross, T.; Beller, M. *Science* **2002**, *297*, 1676.
- (111) Fuchs, D.; Rousseau, G.; Diab, L.; Gellrich, U.; Breit, B. *Angew. Chem., Int. Ed.* **2012**, *57*, 2178.
- (112) Milstein, D.; Huckaby, J. L. *J. Am. Chem. Soc.* **1982**, *104*, 6150.
- (113) Beller, M.; Cornils, B.; Frohning, C. D.; Kohlpainter, C. W. *J. Mol. Catal. A* **1995**, *104*, 17.
- (114) Burke, P. M. *Hydrocarboxylation of butadiene to 3-pentenoic acid*. U.S. Patent 4,622,423, November 11, 1986.
- (115) Beller, M.; Krotz, A.; Baumann, W. *Adv. Synth. Catal.* **2002**, *344*, 517.
- (116) Mika, L. T.; Tuba, R.; Tóth, I.; Pitter, S.; Horváth, I. T. *Organometallics* **2011**, *30*, 4751.
- (117) Seayad, A.; Jayasree, S.; Damodaran, K.; Toniolo, L.; Chaudhari, R. V. *J. Organomet. Chem.* **2000**, *601*, 100.
- (118) Clegg, W.; Eastham, G. R.; Elsegood, M. R. J.; Tooze, R. P.; Wang, X. L.; Whiston, K. *Chem. Commun.* **1999**, 1877.
- (119) Clegg, W.; Eastham, G. R.; Elsegood, M. R. J.; Heaton, B. T.; Oggi, J. A.; Tooze, R. P.; Whyman, R.; Zacchini, S. *J. Chem. Soc.; Dalton Trans.* **2002**, 3300.
- (120) Wolowska, J.; Eastham, G. R.; Heaton, B. T.; Iggo, J. A.; Jacob, C.; Whyman, R. *Chem. Commun.* **2002**, 2784.
- (121) de la Fuente, V.; Waugh, M.; Eastham, G. R.; Iggo, J. A.; Castellón, S.; Claver, C. *Chem.—Eur. J.* **2010**, *16*, 6919.
- (122) Nozaki, K.; Sato, N.; Tonomura, Y.; Yasutomi, M.; Takaya, H.; Hiyama, T.; Matsubara, T.; Koga, N. *J. Am. Chem. Soc.* **1997**, *119*, 12779.
- (123) Nozaki, K.; Sato, N.; Takaya, H. *J. Am. Chem. Soc.* **1995**, *117*, 9911.
- (124) Iggo, J. A.; Kawashima, Y.; Liu, J.; Hiyama, T.; Nozaki, K. *Organometallics* **2003**, *22*, 5418.